Indian Journal of Chemistry
Vol. 55A, August 2016, pp. 938-949

Structure and reactivity of di-*n*-butyltin(IV) derivative of chlordiazepoxide based on electronic structure calculations

Sandeep Pokharia[a,*], Rachana Joshi[a], Mamta Pokharia[a], Swatantra Kumar Yadav[b] & Hirdyesh Mishra[b]

[a]Organometallics and Molecular Modelling Group, Chemistry Section, Mahila Mahavidyalaya, Banaras Hindu University, Varanasi 221 005, India

Email: sandeepp@bhu.ac.in

[b]Physics Section, Mahila Mahavidyalaya Banaras Hindu University, Varanasi 221 005, India

Received 28 December 2015; revised and accepted 27 July 2016

Density functional theory calculations in electronic structure studies of *n*-Bu_2SnL_2 (where L is the monoanion of chlordiazepoxide (LH), a benzodiazepine derivative with hypnotic action) have been reported using the Gaussian09 software. The molecular geometries of LH and tetrahedral *n*-Bu_2SnL_2 have been optimized at B3LYP/6-31G(d,p) and B3LYP/ 6-31G(d,p)/Def2-SVP(Sn) level of theory, respectively. Harmonic vibrational frequencies are computed at the same level of theory to find the true potential energy surface minima. The effect of functional, basis set and computational cost is analyzed. The various geometrical and thermochemical parameters have been obtained in gas phase and in the solvent. The atomic charges at all the atoms are calculated using Mulliken population analysis, Hirshfeld population analysis and natural population analysis. The charge distribution within the studied complex is explained on the basis of molecular electrostatic potential maps, and conceptual-DFT based global reactivity descriptors using the finite difference approximation method. The calculated parameters suggest a distorted tetrahedral geometry around the central Sn atom. The calculated Sn–O bond lengths reveals different degree of interaction of two chlordiazepoxide units with the di-*n*-butyltin(IV) moiety. Among the atoms coordinated to the central Sn atom, oxygen from one LH unit is nucleophilic, whereas the second oxygen atom from the other LH unit is electrophilic in nature. The results provide an insight into the efficacy of computational methods in understanding the structure and reactivity of organotin(IV) derivatives of hetero donor atoms.

Keywords: Theoretical chemistry, Density functional calculations, Electronic structures, Global reactivity descriptors, Organotin compounds, Tin, Chlordiazepoxide

The contemporary research has drawn considerable research interest in organotin(IV) compounds due to their structural diversity, apart from their wide range of industrial and biological applications.[1] These compounds are characterized by the presence of tetravalent Sn centres and at least one covalent Sn–C bond. Most significantly, they often form structures in which previously tetravalent Sn atoms become hypervalent, owing to the large size of Sn-atom and the availability of low lying empty 5*d* atomic orbitals.[2] In such cases, the Sn atoms are involved in additional inter- and/or intra-molecular interactions that expand their coordination number, and the appearance of such additional interactions results from the pronounced electron-acceptor ability of the Sn atoms. In the presence of electron donors which can provide a lone electron pair to the Sn atom, these interactions get strengthened and lead to the formation of coordination (dative) bonds. Apart from these unique structural features, more recently organotin(IV) compounds have found possible use as potential biologically active non-platinum chemotherapeutic metallopharmaceuticals possessing anti-tumour activity.[3–7] The speciation of the organotins in the biological systems has revealed that the biological activity of these compounds may be due to the presence of easily hydrolysable groups (easily dissociable chelating ligands), yielding intermediates, such as $R_nSn^{(4-n)+}$ (n = 2 or 3 moieties), number of Sn–C bonds, electronic and geometrical properties, mode of coordinating ligands and the structure of organotin(IV) complex.[2] For instance, it has been suggested[8] that for antiproliferative activity, the organotin(IV) compounds should possess available coordination positions at Sn centre and relatively stable ligand–Sn bonds (for e.g., Sn–N and Sn–S) as well as their slow hydrolytic decomposition.

The organotin(IV) complexes with active drugs as ligands have emerged as an approach to new drug development with the goal to prepare compounds with better or different pharmacological profile than that of

the free ligand, as the biological activity of the organic drug can be enhanced by masking it upon coordination to an organotin(IV) moiety. In the last two decades, the investigations on organotin(IV)-drug system have been carried out extensively with the drugs having hetero donor atoms (N/O/S) such as, non-steroidal anti-inflammatory drugs (NSAIDs),[9–14] antibiotics,[15] quinolone antibacterials,[15,16] anti-hypertensive drugs,[17] and antivirals,[18] so as to design new metallopharmaceuticals with different pharmacological profile. A few among these studied organotin(IV) complexes have been reported to exhibit good *in vitro* anticancer,[14,15,18] antituberculosis,[10,13] and antiviral activities.[15,18] Recently,[19] a series of organotin(IV) complexes of chlordiazepoxide (LH, Fig. 1(a)), a benzodiazepine derivative with anticonvulsant and hypnotic properties, which acts on benzodiazepine allosteric sites that are part of the $GABA_A$ receptor/ion-channel complex thereby producing inhibitory effects on the central nervous system and body,[20] have been synthesized, spectroscopically characterized, and their potential biological application has been analysed by screening against several antibacterial indictor strains. For instance, its di-*n*-butyltin(IV) complex exhibited good inhibition against *Escherichia Coli* and *Vibrio Cholera*.[19] However, the structure activity relationship of these synthesized complexes in terms of their electronic structure has not been highlighted, though the density functional theory (DFT) calculations based quantum-chemical methods can well be utilized to correlate the electronic structure properties of a particular system with its potential biological activity.

The geometric structures of several organotin(IV) derivatives with ligands containing hetero donor atoms such as N/O/S are credibly represented by quantum-chemical calculations performed within a domain of DFT, owing to the fact that DFT-based methods represents a reasonable approach to take into account the electron correlation for such systems.[21–25] However, the structural analysis based on conceptual-DFT based reactivity descriptors is hardly reported. Nevertheless, the study of these descriptors to comprehend the electronic structure of an organotin(IV) complex which has far reaching consequences on its interaction with macromolecular receptors is indispensable for the design of new metallopharmaceuticals. Further, in an attempt to design new molecular entities possessing unique structural features and broad range of biological activity, we have systematically initiated efforts on organotin(IV)-drug systems. However, in order to gain a better insight into the physicochemical and biological properties of organotin(IV) complexes with drugs a thorough knowledge of their electronic and geometric molecular structures is significant. As a part of our continuing work on structure and reactivity study of organotin(IV)-drug system in the light of conceptual-DFT based quantum-chemical calculations,[26] the present work highlights the theoretical investigation based on an appropriate DFT method for di-*n*-butyltin(IV) derivative of chlordiazepoxide (*n*-Bu_2SnL_2, where L is the monoanion of chlordiazepoxide) (Fig. 1(b)). The conceptual-DFT based global reactivity descriptors thus calculated are interpreted in terms of electronic distribution within the complex to account for its binding towards macromolecular receptors.

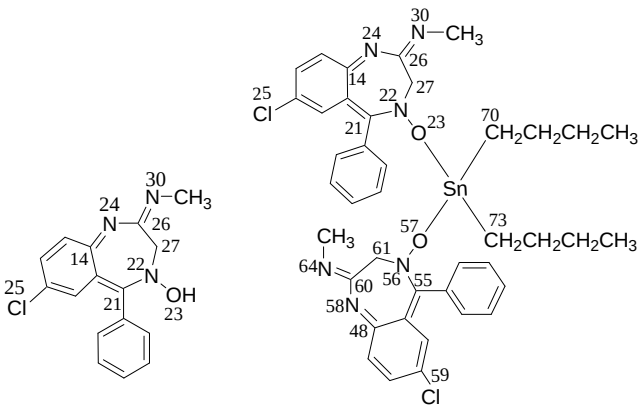

(a) **(b)**

Fig. 1**–**Structure (along with atom number) of (a) chlordiazepoxide (LH), and, (b) di-*n*-butyltin(IV) derivative of chlordiazepoxide.

Theoretical

DFT is a theory of electronic ground state structure, embedded in terms of electronic density distribution ($\vec{r}$), which holds significance for the understanding and calculation of the ground state density, ($\vec{r}$), and energy, *E*, of the molecules, clusters, and solids- any system consisting of nuclei and electrons- with or without applied static perturbations.[27] Within the domain of DFT, conceptual-DFT (or chemical reactivity theory) attempts to delineate and explicate important universal concepts of molecular structure and molecular reactivity.[28] The conceptual-DFT based global reactivity descriptors considered in the present study are given below.

Electronic chemical potential ( ), which measures the sensitiveness of the system's energy *E* to a change in number of electrons *N*:[29]

$$\mu = \left(\frac{\partial E}{\partial N}\right)_{v(\vec{r})} \quad \ldots (1)$$

The finite-difference approximation, alongwith the Koopman's approximation, gives in terms of the energies of frontier molecular orbitals as: [28]

$$\mu = \frac{E_{LUMO} + E_{HOMO}}{2} \quad \ldots (2)$$

where, E_{HOMO} is the energy of the highest occupied molecular orbital and E_{LUMO} is the energy of the lowest unoccupied molecular orbital.

Global hardness ( ), a global property is regarded as a resistance to charge transfer, and can be defined as:[30]

$$\eta = \left(\frac{\partial^2 E}{\partial N^2}\right)_{v(\vec{r})} = \left(\frac{\partial \mu}{\partial N}\right)_{v(\vec{r})} \quad \ldots (3)$$

The finite-difference approximation, alongwith the Koopman's approximation, gives in terms of the energies of frontier molecular orbitals as:[28]

$$\eta = E_{LUMO} - E_{HOMO} \quad \ldots (4)$$

Global softness (S), measures the ease of charge transfer and is associated with high polarizability. It can be defined as:[27,31]

$$S = \frac{1}{\eta} = \left(\frac{\partial N}{\partial \mu}\right)_{v(\vec{r})} \quad \ldots (5)$$

Electrophilicity index ( ), measures the electrophilic power of an electrophile (ligand) to stabilize a covalent (soft) interaction on the basis of lowering of the total binding energy upon partial electron transfer (with maximal flow) between an electron donor and an electron acceptor.[28,32] The electrophilicity of the ligand can be expressed as:

$$\omega = -\Delta E \equiv \frac{\mu^2}{2\eta} \quad \ldots (6)$$

where, $-\Delta E$ is the change in the electronic energy.[28,32,33]

Computational details

All the quantum chemical calculations have been performed using the Gaussian 09 program package.[34] The molecular geometries of LH and *n*-Bu_2SnL_2 were fully optimized in the gas phase as well as in solution at the DFT level using the B3LYP functional which is a combination of Becke's three parameter (B3) gradient corrected hybrid exchange functional (which includes a mixture of Hartree-Fock exchange with DFT exchange-correlation)[35] with the dynamical correlation functional of Lee, Yang and Parr (LYP) (which includes both local and non-local correlation provided by LYP expression and VWN correlation functional (functional III) for required excess local correlation).[36,37] All the atoms except Sn were described by 6-31G(d,p) basis set, which is a double zeta split valence polarized basis set of contracted Gaussian-type function with d-type Cartesian-Gaussian polarization functions added to each heavy atoms and p-type polarization functions to hydrogen atoms. This basis set contains a reasonable number of basis set functions that are able to reproduce the experimental observations and led to accurate predictions on geometric parameters of organic parts of the organometallic systems.[38] The Sn atom in *n*-Bu_2SnL_2 was described by two different basis sets. The first one consists of Ahlrich's basis set in its Def2-SVP version developed by Weigend,[39] in which the inner core shells of Sn ($1s^2 2s^2 2p^6 3s^2 3p^6 3d^{10}$) were described using the effective core potential of the Stuttgart group (ECP28MDF),[40] and outer shells were described by (10*s*7*p*6*d*)/[4*s*4*p*2*d*]. The second basis set consists of LANL2DZ in which Sn inner shells are described by effective core potential ECP46MWB ($1s^2 2s^2 2p^6 3s^2 3p^6 3d^{10} 4s^2 4p^6 4d^{10}$) along with the basis set (3*s*3*p*)/[2*s*2*p*].[41] All the parameters of the basis sets and core potentials for Def2-SVP basis set were taken from the EMSL basis set exchange.[42,43] The molecular geometry of *n*-Bu_2SnL_2 was also optimized using four more DFT methods: M06-2X (a hybrid functional),[44] Cam-B3LYP (a hybrid-exchange correlation functional which is a long range corrected version of B3LYP using the coulomb-attenuating method),[45] PBEPBE (a gradient corrected hybrid correlation functional),[46] and B3PW91 (a gradient-corrected correlation functional which specifies Becke Three Parameter Hybrid Functional with the non-local correlation provided by Perdew/Wang 91),[47] as implemented in the Gaussian 09 program package. All the calculations presented in this work were carried out without any symmetry constraint at B3LYP/6-31G(d,p)/Def2-SVP(Sn) level of theory. The geometry optimization was carried out through an algorithm of iterative steps to locate true global minima on the potential energy surface (PES) with default parameters for convergence is met. The absence of an imaginary frequency in a harmonic frequency calculation carried out at the same level of theory indicates that the calculated geometry is a true global minimum on the PES. The optimized geometrical parameters and the atomic charges at all

the atoms in the studied systems were calculated using Mulliken population analysis (MPA), Hirshfeld population analysis (HPA), and natural population analysis (NPA) at the same level of theory. The energies of frontier molecular orbitals have been calculated using finite difference approximation (whereby, single point energy calculation was performed on the previously optimized geometry for the neutral (N), cationic (N–1) and anionic (N+1) systems).[28,48] The conceptual-DFT based global reactivity descriptors, as described under theoretical background, have been calculated for the studied systems, based on MPA, HPA and NPA, using finite difference approximation. The bulk solvent effect (water as solvent) has been included through integral equation formalism variant of polarizable continuum model (IEF-PCM) method, which creates the solute cavity via a set of overlapping spheres and computes the energy in solution by making the solvent reaction field self-consistent with the solute electrostatic field.[49] The molecular electrostatic potential maps and visualization of all results have been performed using Gauss View 5.0.[50]

Results and Discussion

The DFT based quantum chemical studies on *n*-Bu_2Sn(IV) derivative of chlordiazepoxide have been successfully accomplished in the gas phase and in the presence of solvent with the methods mentioned above in the computational details. In order to search a computationally economic and viable method for the electronic structure calculations of *n*-Bu_2SnL_2, a comparative analysis of the performance of various basis sets and functionals has been carried out and the results are presented in Table S1 (Supplementary Data). The results indicate that all the functionals and basis sets satisfactorily describe the molecular geometry of the studied derivative, though small differences are evident.

The electronic structure calculation of *n*-Bu_2SnL_2 in gas phase was successfully achieved with different functionals, as mentioned in computational details. Since the crystal structure parameters for the *n*-Bu_2SnL_2 are not available, hence in order to validate the efficacy of the method employed, the reported Sn–O bond length,[9,51,52] for other di-*n*-butyltin(IV) derivatives of drugs having oxygen as a coordinating atom has been taken as a reference. As evident from the results (Table S1), except Hartree-Fock (HF), all other functionals gave similar degree of divergence. Further, with a particular combination of the basis set the minimum energy structure on the PES obtained upon geometry optimization is always attained with the hybrid functional B3LYP, indicating that among the studied methods B3LYP functional gives the most stable structure (most negative E_{SCF} in absolute terms). Likewise with a particular combination of the basis set, the maximum calculated dipole moment is always obtained with M06-2X functional. Furthermore, with all the studied functionals the two calculated Sn–O bond lengths are not equal, indicating that the two chlordiazepoxide units in *n*-Bu_2SnL_2 have different degree of interactions with the *n*-Bu_2Sn(IV) moiety. Similar trend is observed for all other significant bond distances and various geometrical parameters. Most significantly, the calculated Sn–O bond length in *n*-Bu_2SnL_2 with the chlordiazepoxide units, 2.08±0.06 Å, is closer to the values reported for other systems.[51,52]

The effect of basis set

The calculations for *n*-Bu_2SnL_2 in gas phase have been successfully performed with different combinations of basis set, as mentioned in computational details. All the studied basis sets gave similar quality of results (Table S1). As evident from the results, with a particular functional, the minimum energy structure on the PES obtained upon geometry optimization is always attained upon addition of polarization functions to all the atoms except Sn atom, irrespective of the type of basis set used to define the Sn atom. Further, with a particular functional and basis set for all the elements (except Sn), the minimum energy structure on the PES is always attained with Def2-SVP basis set. Furthermore, with a particular functional the application of larger basis sets containing polarization functions to all the atoms, except Sn atom, lengthens the two calculated Sn–O bond lengths closer to the reported values for other systems.[9,51,52] The results obtained with 6-31G(d,p)/ Def2-SVP(Sn) basis set are most appropriate regardless of the DFT method used, as this combination of basis sets alongwith B3LYP functional gave calculated Sn–O bond lengths closer to the reported values.

The results, thus, indicate that irrespective of the basis set used, the performance with B3LYP method is the best among the functionals considered for the present study, and hence all of the study for *n*-Bu_2SnL_2 has been performed at B3LYP/ 6-31G(d,p)/Def2-SVP(Sn) level of theory. The functional B3LYP has been credibly reported

previously for the electronic structure calculations of several organotin(IV) derivatives with hetero donor atoms.[21–26]

Geometry optimization

The theoretical studies on chlordiazepoxide (LH) have been accomplished at B3LYP/6-31G(d,p), whereas that on *n*-Bu_2SnL_2 have been accomplished using Hartree-Fock (HF) and different DFT methods with different combinations of basis sets as mentioned in computational details. The selected bond lengths and bond angles in the studied systems calculated using respective methods at 6-31G(d,p)/Def2-SVP(Sn) level of theory are presented in Table S2 (Supplementary Data). Since the B3LYP/6-31G(d,p)/Def2-SVP(Sn) method has been considered an appropriate method for the study of *n*-Bu_2SnL_2, the results are thus discussed at this level of theory only. The ground state optimized geometries in the gas phase for LH and *n*-Bu_2SnL_2 are presented in Fig. 2 (*cf.* Fig. 1 for atom number notation). As evident from the results (*cf.* Table S2), the calculated Sn–O bond lengths in *n*-Bu_2SnL_2 are 2.117 Å and 2.065 Å, respectively for O23 and O57, signifying that the two chlordiazepoxide units have different degrees of interaction with the *n*-Bu_2Sn(IV) moiety in *n*-Bu_2SnL_2. Moreover, these values correspond largely to the single covalent radius value of *ca.* 2.0 Å, and compare well with those found in other organotin(IV) complexes with oxygen atom as donor atom.[9,10,13,14,51,52] Likewise, the calculated Sn–C bond lengths in *n*-Bu_2SnL_2, viz. Sn–C70 and Sn–C73 are 2.192 Å and 2.177 Å, respectively, which are in accordance with the values reported for organotin(IV)-drug systems with oxygen as coordinating atom.[9,10,13,51,52] Further, the calculated bond angles around the central Sn atom in *n*-Bu_2SnL_2 indicates a distorted tetrahedral arrangement of two butyl groups and two chlordiazepoxide units coordinating through deprotonated oxygen atoms, as reported previously.[19]

Thermochemical studies

The various energetic and thermochemical parameters for LH and *n*-Bu_2SnL_2 both in the gas phase and in the solvent field have been obtained at 1 atm and 298.15 K at B3LYP/6-31G(d,p) and B3LYP/6-31G(d,p)/Def2-SVP(Sn) level of theory, respectively, and the results are presented in Table S3 (Supplementary Data). The rotational temperature ($_r$) is useful in deciding whether a molecule will show classical or quantum behaviour depending on the temperature.[53] Since for both LH and *n*-Bu_2SnL_2, T >> $_r$ (*cf.* Table S3), these molecules will show classical behaviour. Further, the zero point vibrational energy (ZPVE) is the difference in the energy of the bottom of the internuclear potential energy well (V_{BOT}) and the energy of the vibrational ground state (v = 0).[53,54] The calculated ZPVE for LH and *n*-Bu_2SnL_2 in gas phase is 170.08 kcal/mol and 480.88 kcal/mol, respectively, which gets lowered for both LH and *n*-Bu_2SnL_2 in the solvent field (*cf.* Table S3), indicating that vibrational ground state (v = 0) gets stabilized in the solvent field. Furthermore, the total energy of LH and *n*-Bu_2SnL_2 in gas phase as well as in the solvent field has been calculated after zero-point correction, and thermal correction to energy, enthalpy and Gibbs free energy, and the results indicate that all of the electronic energy of LH and *n*-Bu_2SnL_2 is exothermic. For instance, the calculated total (*cf.* Table S3) energy of *n*-Bu_2SnL_2 after thermal correction to Gibbs free energy is

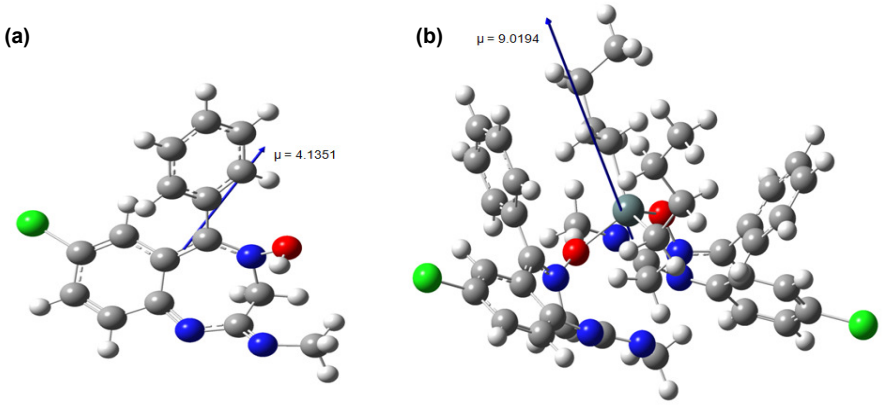

Fig. 2–Ground state optimized geometry (in gas phase) of (a) chlordiazepoxide (LH) calculated at B3LYP/6-31G(d,p) level of theory, and, (b) *n*-Bu_2SnL_2 calculated at B3LYP/6-31G(d,p)/Def2-SVP(Sn) level of theory.

–3163.638622 a.u., which further decreases to –3163.674822 a.u. in the solvent field, indicating the stabilization of the complex (–22.72 kcal/mol) in the solvent field.

The number of thermally accessible energy levels at a given temperature is represented by total partition function. Since, an individual molecule in an ideal gas has energy due to the different types of motion, viz., translation (E_{trans}), rotation (E_{rot}) and vibration (E_{vib}), as well as due to its electronic state (E_{elec}), therefore assuming these four processes as independent, the total partition function for a molecule has contributions from each of these form of energy as:[53,54]

$$q(V,T) = q^E q^T q^R q^V \quad \ldots (7)$$

where, q^E is the electronic, q^T is translational, q^R is rotational and q^V is vibrational partition function. The partition function from each component can thus be used to determine the contribution to internal thermal energy (E_{tot}), entropy (S_{tot}) and constant volume molar heat capacity (CV_{tot}). The electronic heat capacity and the internal thermal energy due to electronic motion are both zero, because electronic partition function does not contain temperature dependent terms. The value of E_{tot}, S_{tot} and CV_{tot} for *n*-Bu_2SnL_2 in gas phase is 513.182 kcal/mol, 304.108 cal/mol/K and 193.07 cal/mol/K, respectively (*cf.* Table S3). As evident from the results, the maximum contribution to E_{tot}, S_{tot} and CV_{tot} of LH as well as *n*-Bu_2SnL_2 in gas phase and in the solvent field is due to vibrational motion of the molecule. Further, the individual contribution due to each component to the partition function has also been calculated for LH and *n*-Bu_2SnL_2 in gas phase and in the solvent field. The results indicate that the maximum contribution is due to vibrational partition function computed with the zero of energy being the bottom of the well ($q_{vib, BOT}$). In *n*-Bu_2SnL_2, in the gas phase the q^E, q^T, q^R, $q^{V,BOT}$ and $q^{V,v=0}$ contribution to the total molecular partition function is 10^0, $10^{8.972}$, $10^{8.016}$, $10^{-310.138}$ and $10^{42.346}$, respectively (*cf.* Table S1), whereas in the solvent field the contribution from these components is 10^0, $10^{8.972}$, $10^{8.026}$, $10^{-309.786}$ and $10^{42.543}$, respectively. These results reveal that in the solvent field, the contribution due to q^R and $q^{V,v=0}$ increases, whereas that due to $q^{V,BOT}$ decreases, which indicates that in the solvent field the number of thermally accessible rotational and ground vibrational level is increased. Moreover, the free energy of the solvation (ΔG^o_{sol}) for *n*-Bu_2SnL_2 is estimated to be –31.39 kcal/mol.

Atomic charges

The calculation of effective atomic charges plays a significant role in the application of quantum-chemical calculations to molecular systems, since they affect dipole moment, molecular polarizability, electronic structure, acidity-basicity behaviour and several properties of molecular systems. In molecular systems, the attribution of net atomic charges is allowed by population analysis, though the atomic charge is not a physical reality.[55] Since, in quantum mechanics neither an atom nor an atomic charge in a molecule is observable, therefore different mathematical treatments can be applied to assign a function of the electron density to a particular atom, and, hence based on limitations of each method, the results obtained should be carefully analysed. Though, MPA is the most common population analysis method, but it is known to be quite inaccurate, sensitive to conformational equilibriums and strongly dependent on the choice of the basis set; more reliable and robust values are obtained from HPA and NPA.[55] The electron density distribution analysis has been performed on the basis of atomic charges determined by three different population schemes, viz., MPA, HPA and NPA in the gas phase within the LH and *n*-Bu_2SnL_2, respectively, at B3LYP/6-31G(d,p) and B3LYP/6-31G(d,p)/Def2-SVP(Sn) level of theory. The calculated atomic charges based on MPA, HPA and NPA at the selected atoms in *n*-Bu_2SnL_2 are presented in Fig. 3, and

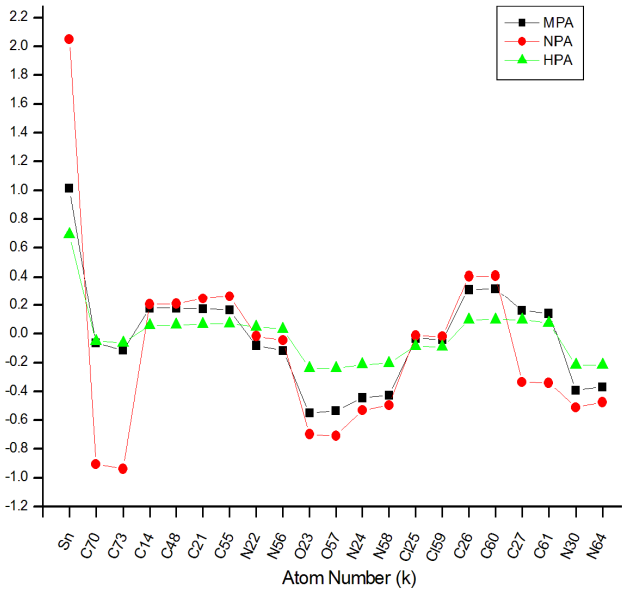

Fig. 3–Plot of atomic charges at the selected atoms of *n*-Bu_2SnL_2 based on MPA, NPA and HPA calculated at B3LYP/6-31G(d,p)/Def2-SVP(Sn) level of theory.

calculated atomic charges along with the population at the selected atoms of LH and *n*-Bu_2SnL_2 are tabulated, respectively in Tables S4, S5 and S6 (Supplementary Data). The population of the atomic orbitals suggest that in *n*-Bu_2SnL_2 the natural electron configuration of central Sn atom is [core]$5s^{1.10}5p^{0.84}5d^{0.01}p^{0.01}$, which differs significantly from *n*-$Bu_2Sn(IV)^{2+}$ cation configuration [core]$5s^2$. The absolute value of the natural charge of Sn in *n*-Bu_2SnL_2 is about 2.049 (*cf.* Table S6) on the basis of NPA, whereas on the basis of MPA and HPA the charge is about 1.016 (*cf.* Table S4) and 0.693 (*cf.* Table S5), respectively. The NPA charge suggests that charge transfer is very minor and interaction of *n*-$Bu_2Sn(IV)$ moiety and two chlordiazepoxide units is mostly ionic. Similar results are reported for diorganotin(IV) systems with ligands having hetero donor atoms.[22,24] Further, the natural electron configuration of coordinating oxygen atoms in two chlordiazepoxide units, viz., O23 and O57 is [core]$2s^{1.75}2p^{4.94}3p^{0.01}3d^{0.01}$ and [core]$2s^{1.75}2p^{4.95}3p^{0.01}$, respectively. The absolute value of natural charge of O23 and O57 on the basis of NPA is –0.698 and –0.708, respectively (*cf.* Table S6), whereas the charge on these atoms on the basis of MPA (*cf.* Table S4) is about –0.549 and –0.533, respectively, and on the basis of HPA (*cf.* Table S5) it is about –0.238 and –0.240, respectively. Moreover, the natural electron configuration of two carbon atoms (covalently bonded to the central Sn atom), viz., C70 and C73 is [core]$2s^{1.16}2p^{3.72}3p^{0.01}$ and [core]$2s^{1.17}2p^{3.75}3p^{0.01}$, respectively. The absolute value of natural charge of C70 and C73 on the basis of NPA is –0.906 and –0.937, respectively (*cf.* Table S6), whereas the charge on these atoms on the basis of MPA (*cf.* Table S4) is about –0.064 and –0.113, respectively, and on the basis of HPA (*cf.* Table S5) it is about –0.051 and –0.065, respectively. The existence of such oppositely charged centres around the central Sn atom further confirms the ionic interaction in the Sn–O bond, resulting in the existence of dative Sn←O bonds. Such an ionic interaction in *n*-Bu_2SnL_2 may lead to slow hydrolytic decomposition of Sn–O bond, suggesting that the complex can exhibit potential antiproliferative activity owing to the existence of *n*-$Bu_2Sn(IV)^{2+}$ moiety in the biological system.

Molecular electrostatic potential (MEP)

The MEP, $V(\vec{r})$ that is created in the space around a molecule by its nuclei and electrons is related to the electron density. It is a significant descriptor that has provided substantial insight of the sites within the molecule where the electron distribution effect is dominant, for instance, for the intermolecular association and molecular properties of small molecules and actions of drug molecules and their analogues,[56] and predicting molecular reactive behaviour.[57] Thus, it is a useful indicator of the sites or regions of a molecule to which an approaching electrophile is initially attracted, and also to the study of interactions that involve a certain optimum level of orientation of the reactants, for instance analysing processes based on the 'recognition' of one molecule by another, such as between a drug and its cellular receptor because it is through their potentials that the two species first 'see' each other.[57] For a system with an electron density function $\rho\left(\vec{r'}\right)$, the MEP at any point $(\vec{r})$ is given rigorously as:[57]

$$V(\vec{r}) = \sum_A \frac{Z_A}{|R_A - (\vec{r})|} - \int \frac{\rho(\vec{r'})d\vec{r'}}{|(\vec{r'}) - (\vec{r})|} \quad \ldots (8)$$

where Z_A is the charge on the nucleus A, located at $\overrightarrow{R_A}$. The summation runs over all the nuclei A in the molecule, with polarization and reorganization effects neglected. The first term which represents the contribution of the nuclei is a positive quantity, whereas the second term accounts for the effect of the electrons and is a negative quantity. Since the MEP surfaces illustrates the charge distribution of the molecules three dimensionally, its significance lies in the fact that apart from visualization of variably charged regions of a molecule it simultaneously displays molecular size, shape and electrostatic potential regions (positive, negative and neutral) in terms of colour grading.[58] The information obtained from the charge distribution of MEP can thus be utilized to understand the interaction between the molecules and to determine the nature of the chemical bond. The MEP surface of chlordiazepoxide (LH) and *n*-Bu_2SnL_2 calculated on the ground state optimized geometries in gas phase at B3LYP/6-31G(d,p) and B3LYP/6-31G(d,p)/Def2-SVP(Sn) level of theory, respectively are presented in Fig. 4. The colour code of these maps is in the range between –0.0838 a.u. (deepest red) and 0.0838 a.u. (deepest blue). An analysis of the MEP map suggests that in LH, the negative region (red coded regions) of the entire molecule is localized around the oxygen atom (O23) and larger parts of the molecule are of intermediary potential. In *n*-Bu_2SnL_2, the negative regions of the

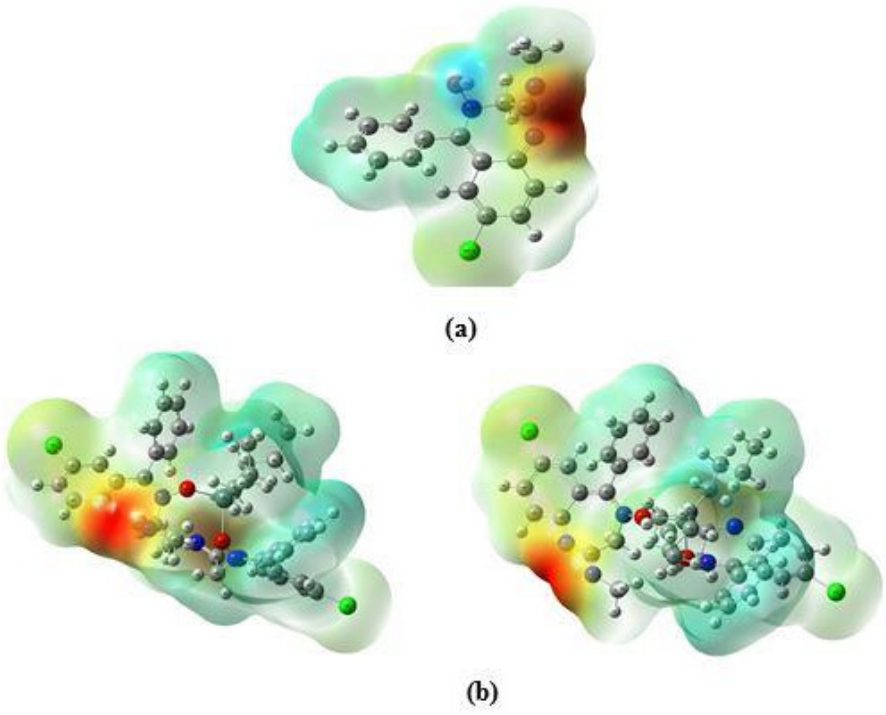

Fig. 4–Molecular electrostatic potential map for ground state optimized geometry (in gas phase) of (a) chlordiazepoxide (LH) calculated at B3LYP/6-31G(d,p) level of theory, and, (b) *n*-Bu_2SnL_2 calculated at B3LYP/6-31G(d,p)/Def2-SVP(Sn) level of theory (red coded and bluish-green coded regions are represented separately).

entire molecule are localized around the hetero atoms in the chlordiazepoxide unit O57 as a coordinating atom, and the positive regions (bluish-green coded regions) of entire molecule are localized in the chlordiazepoxide unit with O23 as a coordinating atom. Further, in *n*-Bu_2SnL_2 relative to the central Sn atom, the region in close proximity to the bonded oxygen atoms (O23 and O57) has excess charge density. These results indicate that upon complex formation, the intramolecular distribution of charge density creates an electropositive centre at the central Sn atom. The MEP maps suggest that an unsymmetrical charge distribution in the *n*-Bu_2SnL_2 may lead to easy transportation of the complex within the biological system and also creates a charge deficient centre at the central Sn atom which can lead to its potential biological activity.

Conceptual-DFT based global reactivity descriptors

The global reactivity descriptors measures the overall reactivity of a molecule and can be considered as response functions describing the system's response to perturbations in number of electrons (N) of a system at constant external (i.e., the potential acting on an electron at the position $\vec{r}$ due to the nuclear attraction along with the other external forces that may be present in the system) potential $v(\vec{r})$. The molecular properties and conceptual-DFT based global reactivity descriptors for the ground state optimized geometries (in the gas phase and in solvent field) of chlordiazepoxide (LH) and *n*-Bu_2SnL_2, calculated using finite difference approximation are presented in Table 1. The results indicate that the dipole moment that accounts for the existence of charged separated regions within the system is greater for *n*-Bu_2SnL_2 (9.0194 Debye) in comparison to LH (4.1351 Debye) in the gas phase, which increases further in the solvent field in both LH and *n*-Bu_2SnL_2. The ionization potential (IP) for *n*-Bu_2SnL_2 (5.9772 eV) is lower than that for LH (6.7451 eV), as also, the electron affinity (EA) for *n*-Bu_2SnL_2 (1.341 eV) which is lower than that of LH (1.0226 eV). As a result, the band gap (ΔE) for *n*-Bu_2SnL_2 (4.636 eV) is lower than that for LH (5.722 eV). In the solvent field, for both LH and *n*-Bu_2SnL_2, the IP decreases whereas EA increases as a result ΔE decreases. Further, the values for all of these parameters in *n*-Bu_2SnL_2 are lower than those in LH. Since the band gap measures the stability and reactivity of the system,[35] therefore, the observed ΔE value indicates that the *n*-Bu_2SnL_2 complex is stable, and a decrease

Table 1–Calculated molecular properties and conceptual-DFT based global reactivity descriptors for the ground state optimized geometries (in gas phase and in solvent field) of chlordiazepoxide (LH) and *n*-Bu_2SnL_2 at B3LYP/6-31G(d,p) and B3LYP/6-31G(d,p)/Def2-SVP(Sn) level of theory, respectively

Parameter / Property	Chlordiazepoxide (LH)		*n*-Bu_2SnL_2	
	Gas phase	Solvent field	Gas phase	Solvent field
E_N (a.u.)[a]	–1317.716063	–1317.732576	–3164.312883	–3164.348319
E_{N+1} (a.u.)	–1317.753644	–1317.822394	–3164.362163	–3164.435812
E_{N-1} (a.u.)	–1317.468186	–1317.546929	–3164.093227	–3164.169722
Dipole moment (Debye)[b]	4.1351	7.888	9.0194	14.684
IP (eV)[c]	6.7451	5.0517	5.9772	4.8599
EA (eV)[d]	1.0226	2.4441	1.3410	2.3808
ΔE (eV)[e]	5.7225	2.6076	4.6362	2.4791
E_{HOMO} (eV)[f]	–6.7451	–5.0517	–5.9772	–4.8599
E_{LUMO} (eV)[g]	–1.0226	–2.4441	–1.3410	–2.3808
(eV)[h]	–3.8839	–3.7479	–3.6591	–3.6204
(eV)[i]	3.8839	3.7479	3.6591	3.6204
(eV)[j]	5.7225	2.6076	4.6362	2.4791
S (eV)[k]	0.1747	0.3835	0.2157	0.4034
(eV)[l]	1.3180	2.6934	1.4440	2.6436

[a]E_N, E_{N+1} and E_{N-1} are the total energies of the system containing respectively, N, N+1 and N–1 electrons; [b]Dipole moment for the system containing *N* number of electrons; [c]IP is the ionization potential given by $E_{N-1} - E_N$; [d]EA is the electron affinity given by $E_N - E_{N+1}$; [e]ΔE is the band gap given by IP–EA; [f]Energy of the highest occupied molecular orbital as $-E_{HOMO}$ = IP; [g]Energy of the lowest unoccupied molecular orbital as $-E_{LUMO}$ = EA; [h]Electronic chemical potential of the system given by ($\frac{E_{HOMO}+E_{LUMO}}{2}$); [i]Electronegativity of the system given by – ; [j]Global hardness of the system given by $E_{LUMO} - E_{HOMO}$; [k]Global softness of the system given by 1/ ; [l]Electrophilicity index of the system given by $^2/2$.

in the band gap upon complexation indicates that *n*-Bu_2SnL_2 is more reactive than LH.

The frontier molecular orbital analysis is significant from the perspective of understanding the distribution of charge density within a system as it helps in estimating the energies and type of frontier molecular orbitals, because these orbitals are the sites of exchange of charge density which leads to the interaction between molecules. The frontier molecular orbital analysis for LH and *n*-Bu_2SnL_2 was performed through the Koopman's approximation within the molecular orbital theory.[28] The E_{HOMO} and E_{LUMO} energies for LH and *n*-Bu_2SnL_2, both in gas phase and in solvent field are presented in Table 1. The E_{HOMO} and E_{LUMO} plots along with the band gap (ΔE) for LH and *n*-Bu_2SnL_2, in the gas phase are presented in Fig. 5. The E_{HOMO} for *n*-Bu_2SnL_2 (–5.9772 eV) is higher than that for LH (–6.7451 eV), and the E_{LUMO} for *n*-Bu_2SnL_2 (–1.341 eV) is lower than that of LH (–1.0226 eV), which indicates that upon complex formation the band gap (ΔE) decreases. Since, when the band gap is large (other things being equal), the system attains high stability and low reactivity, and, when the band gap is small, the system attains low stability and high reactivity,[27] therefore the *n*-Bu_2SnL_2 complex of chlordiazepoxide is more reactive than the ligand itself. Further, as evident from the HOMO and LUMO plots (*cf.* Fig. 5(a)), in LH HOMO is concentrated over the diazepine ring (over N24) and benzene ring (containing Cl25), whereas LUMO is concentrated over N22, O23 and phenyl ring at C21, which indicates the interaction of LH with *n*-Bu_2Sn(IV) moiety through deprotonated oxygen atom, as reported earlier.[19] The HOMO and LUMO plots for *n*-Bu_2SnL_2 presents a distinctive structural feature of the complex. In *n*-Bu_2SnL_2, the HOMO is concentrated over the chlordiazepoxide unit with O57 as a coordinating atom, whereas the LUMO is concentrated over the second chlordiazepoxide unit with O23 as a coordinating atom (*cf.* Fig. 5(b)), which indicates the different degree of interaction of two chlordiazepoxide units with di-*n*-butyltin(IV) moiety resulting in two unequal Sn–O bond lengths as mentioned above. The frontier orbital analysis further indicates that the studied complex interacts with macromolecular receptors through the central Sn atom upon hydrolysis of two Sn–O bonds.

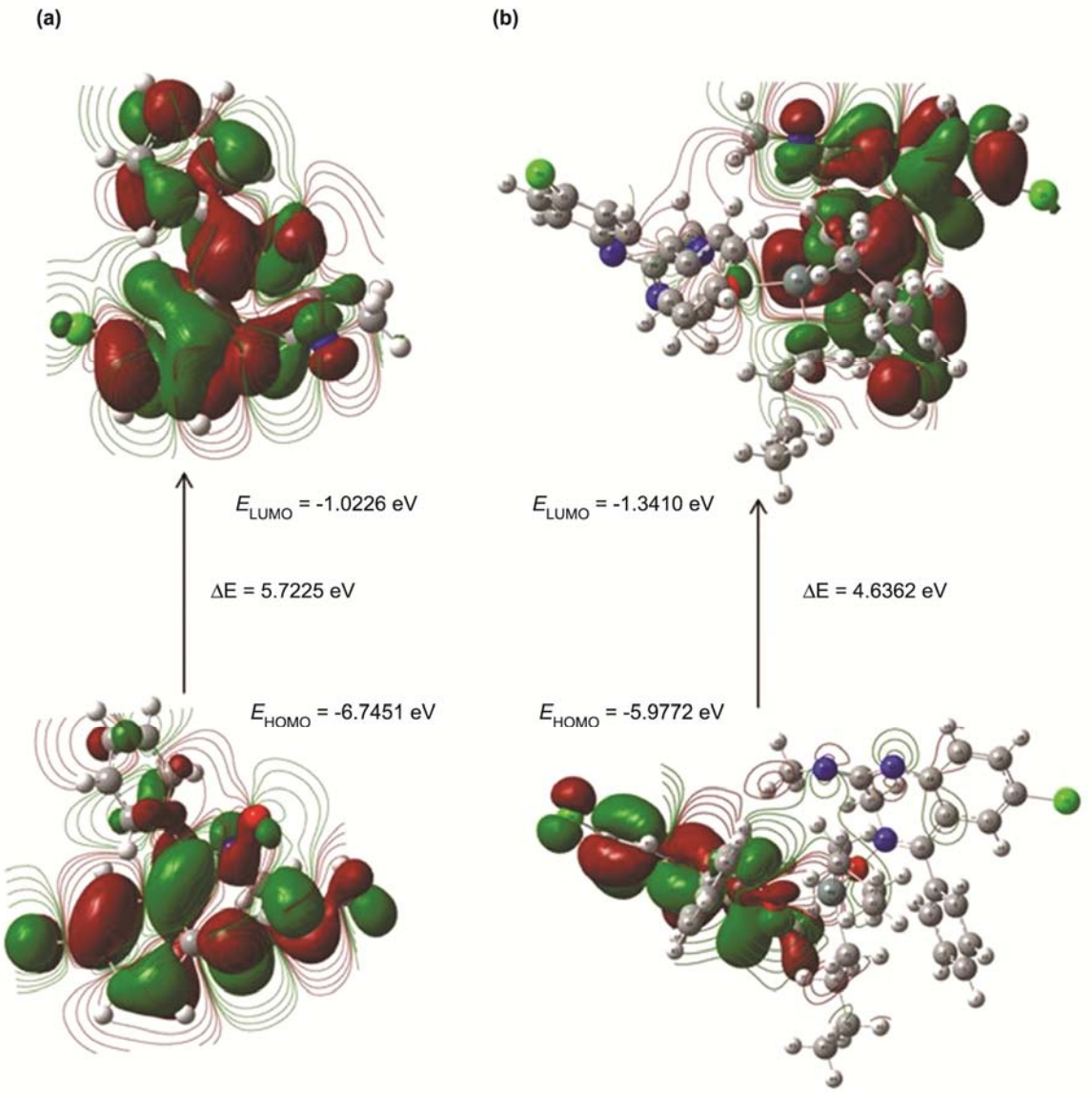

Fig. 5–Highest occupied molecular orbital (HOMO) and lowest unoccupied molecular orbital (LUMO) plots along with band gap (Δ*E*) in the gas phase for (a) chlordiazepoxide (LH) calculated at B3LYP/6-31G(d,p) level of theory, and, (b) *n*-Bu_2SnL_2 calculated at B3LYP/6-31G(d,p)/Def2-SVP(Sn) level of theory.

The global reactivity descriptors calculated based on frontier molecular orbital analysis are electronic chemical potential ( ), electronegativity ( ), global hardness ( ), global softnesss (S) and electrophilicity index ( ). As evident from the results (*cf.* Table 1), the electronic chemical potential ( ) for LH (–3.8839 eV) is greater than that for *n*-Bu_2SnL_2 (–3.6591 eV), which suggests that the energy of the complex is more sensitive towards the change in the number of electrons. Further, since electronegativity ( ) is negative of , it decreases upon complex formation.

Furthermore, global hardness ( ) is a global property that can be regarded as a resistance to charge transfer, whereas global softness (*S*) measures the ease of charge transfer and is associated with high polarizability.[59] The value of for LH (5.7225 eV) is greater than that for *n*-Bu_2SnL_2 (4.6362 eV), whereas the value of S for LH (0.1747 eV) is smaller than that for *n*-Bu_2SnL_2 (0.2157 eV). These values of and S decrease and increase, respectively, in the solvent field (*cf.* Table 1). Since finite difference approximation to global hardness equates it to band

gap (*cf.* Eq. 4), therefore these results indicate that *n*-Bu_2SnL_2 with small band gap is softer and polarizable in comparison to LH. In the presence of solvent, although *n*-Bu_2SnL_2 still remains softer and polarizable as compared to LH, in comparison to the gas phase both LH and *n*-Bu_2SnL_2 becomes softer and more polarizable. Moreover, the electrophilicity index ( ), which measures the electrophilic power of a system,[33,58] and which can be described as the maximum ability of a molecule to accept electrons in the neighbourhood of an electron reservoir,[32,60] has higher value for *n*-Bu_2SnL_2 (1.444 eV) relative to that for LH (1.318 eV). This electrophilic power of both LH and *n*-Bu_2SnL_2 further increases in the solvent field. Since is positive and greater for the complex, therefore the charge transfer (*cf.* Eq. 6) is an energetically favourable process, and assuming both the systems as electron donor, in comparison to LH the complex has a greater electrophilic power during partial electron transfer to an electron acceptor. These results suggest that *n*-Bu_2SnL_2 can exhibit potential antiproliferative activity, because it is soft, polarizable and the charge transfer resulting upon its probable interaction with macromolecular receptor is an energetically favourable process.

Computational cost

In quantum-chemical calculations an important criterion for the applicability of a DFT method is affordability or computational time needed. The scaled CPU time (normalized to PBEPBE/ 6-31G(d,p)/Def2-SVP(Sn)) for single point energy calculation for a particular method used for electronic structure calculation of *n*-Bu_2SnL_2 is given in Table S1. As evident from the results, with a particular functional, application of larger basis sets containing polarization functions to all the atoms, except the Sn atom, increases the computational time. Further, with a particular combination of basis sets, PBEBPBE functional requires minimum computational time. Furthermore, though an improvement in the quality of basis set to 6-31G(d,p)/Def2-SVP(Sn) increases the computational time with all the studied DFT methods, but simultaneously it better describes the energetic and geometrical parameters closer to the reference system.[9,51,52] Hence, a balance between the DFT method chosen and computing time needed is indispensable for the calculation of electronic structure properties of *n*-Bu_2SnL_2.

Conclusions

The present study validates that the theoretical calculations can be successfully performed for di-*n*-butyltin(IV) complex of chlordiazepoxide at B3LYP/6-31G(d,p)/Def2-SVP(Sn) level of theory. This level of theory demonstrates its efficacy over other DFT methods employed as the calculated values for the coordinating bond length and various other geometrical parameters in *n*-Bu_2SnL_2 are closer to those reported for other organotin(IV) complexes with hetero donor atoms. Further, the thermochemical studies performed, successfully calculates total molecular partition function and various thermochemical parameters, indicating that all of the electronic energy of the studied systems is exothermic.

The calculated conceptual-DFT global reactivity descriptors indicate that complexation leads to softness in *n*-Bu_2SnL_2 relative to LH. Further, the charge transfer from the complex is an energetically favourable process and as a result *n*-Bu_2SnL_2 can have greater biological significance, since it provides some insight for its probable interaction with macromolecular receptors in order to explain the biological activity. The theoretical calculations performed have identified the HOMO and LUMO orbitals for LH and *n*-Bu_2SnL_2 based on the frontier molecular orbital analysis. In *n*-Bu_2SnL_2, the HOMO is concentrated over O57 containing chlordiazepoxide unit, whereas LUMO is concentrated over the second chlordiazepoxide unit containing O23 as the coordinating atom. Likewise, the molecular electrostatic potential plots further confirm the charge distribution within the *n*-Bu_2SnL_2 complex. These studies explain the general behaviour of organotin(IV) complexes, in which the Sn centre is found to be electrophilic and also, the coordinating bond lengths are weak enough to undergo slow hydrolysis.

Supplementary Data

Supplementary data associated with this article, i.e., Table S1-S6, are available in the electronic form at http://www.niscair.res.in/jinfo/ijca/IJCA_55A(08)938-949_SupplData.pdf.

References

1 Nath M, *Appl Organometal Chem*, 22 (2008) 598.
2 Pellerito L & Nagy L, *Coord Chem Rev*, 224 (2002) 111.
3 Pellerito C, Nagy L, Pellerito L & Szorcsik A, *J Organomet Chem*, 691 (2006) 1733.
4 Hadjikakou S K & Hadjiliadis N, *Coord Chem Rev*, 253 (2009) 235.

5 Alama A, Tasso B, Novelli F & Sparatore F, *Drug Discov Today*, 14 (2009) 500.

6 Arjmand F, Parveen S, Tabassum S & Pettinari C, *Inorg Chim Acta*, 423 (2014) 26.

7 Carraher C E Jr & Roner M R, *J Organomet Chem*, 751 (2014) 67.

8 Saxena A K & Huber F, *Coord Chem Rev*, 95 (1989) 109.

9 Hadjikakou S K, Demertzis M A, Miller J R & Kovala-Demertzi D, *J Chem Soc, Dalton Trans*, 5 (1999) 663.

10 Kovala-Demertzi D, Dokorou V, Ciunik Z, Kourkoumelis N & Demertzis M A, *Appl Organometal Chem*, 16 (2002) 360.

11 Kovala-Demertzi D, *J Organomet Chem*, 691 (2006) 1767.

12 El-Gamel N E A, *J Coord Chem*, 62 (2009) 2239.

13 Kovala-Demertzi D, Dokorou V, Primikiri A, Vargas R, Silvestru C, Russo U & Demertzis M A, *J Inorg Biochem*, 103 (2009) 738.

14 Dokorou V, Primikiri A & Kovala-Demertzi D, *J Inorg Biochem*, 105 (2011) 195.

15 Roner M, Carraher C E Jr., Roehr J & Bassett K, *J Polym Mater*, 23 (2006) 153.

16 Zhao A, Shahi K R, Roner M R, Barot G, Fiore T, Pellerito C, Scopelliti M, Pellerito L & Carraher C E Jr, *J Polym Mater*, 25 (2008) 87.

17 Jancovics H, Pettinari C, Marchetti F, Kamu E, Nagy L, Troyanov S & Pellerito L, *J Inorg Biochem*, 97 (2003) 370.

18 Carraher C E Jr, Sabir T, Roner M, Shahi K, Bleicher R, Roehr J & Bassett K, *J Inorg Organomet Polym Mater*, 16 (2006) 249.

19 Dhir K, Kaur H, Puri J K & Mittu B, *J Organomet Chem*, 755 (2014) 101.

20 Chweh A Y, Lin Y B & Swinyard E A, *Life Sci*, 34 (1984) 1763.

21 Geerlings P, Vivas-Reyes R, De Proft F, Biesemans M & Willem R, *Metal-Ligand Interactions, NATO Science Series*, Russo N *et al.* (eds.) (The Netherlands: Kluwer Academic Publishers) 2003 p. 461.

22 Girichev G V, Giricheva N I, Koifman O I, Minenkov Y V, Pogonin A F, Semeikin A S & Shlykov S A, *Dalton Trans*, 41 (2012) 7550.

23 Thomas R, Nelson J P, Pardasani R T, Pardasani P & Mukherjee T, *Helv Chim Acta*, 96 (2013) 1740.

24 Latrous L, Tortajada J, Haldys V, Léon E, Correia C & Salpin J –Y, *J Mass Spectrom*, 48 (2013) 795.

25 Matczak P, *Struct Chem*, 26 (2015) 301.

26 Pokharia S, *Res J Chem Sci*, 4 (2014) 56.

27 Kohn W, Becke A D & Parr R G, *J Phys Chem*, 100 (1996) 12974.

28 Geerlings P, De Proft F & Langenaeker W, *Chem Rev*, 103 (2003) 1793.

29 Parr R G, Donnelly R A, Levy M & Palke W E, *J Chem Phys*, 68 (1978) 3801.

30 Parr R G & Pearson R G, *J Am Chem Soc*, 105 (1983) 7512.

31 Yang W & Parr R G, *Proc Natl Acad Sci USA*, 82 (1985) 6723.

32 Parr R G, Szentpály L v & Liu S, *J Am Chem Soc*, 121 (1999) 1922.

33 Chattaraj P K, Sarkar U & Roy D R, *Chem Rev*, 106 (2006) 2065.

34 *Gaussian 09, rev. B.01*, (Gaussian, Inc., Wallingford CT) 2009.

35 Becke A D, *J Chem Phys*, 98 (1993) 5648.

36 Lee C, Yang W & Parr R G, *Phys Rev B*, 37 (1988) 785.

37 Vosko S H, Wilk L & Nusair M, *Can J Phys*, 58 (1980) 1200

38 Francl M M, Pietro W J, Hehre W J, Binkley J S, DeFrees D J, Pople J A & Gordon M S, *J Chem Phys*, 77 (1982) 3654.

39 Weigend F & Ahlrichs R, *Phys Chem Chem Phys*, 7 (2005) 3297.

40 Metz B, Stoll H & Dolg M, *J Chem Phys*, 98 (2000) 2563.

41 Hay P J & Wadt W R, *J Chem Phys*, 82 (1985) 299.

42 Feller D, *J Comput Chem*, 17 (1986) 1571.

43 Schuchardt K L, Didier B T, Elsethagen T, Sun L, Gurumoorthi V, Chase J, Li J & Windus T L, *J Chem Inf Model*, 47 (2007) 1045.

44 Zhao Y & Truhlar D G, *Theor Chem Acc*, 120 (2008) 215.

45 Yanai T, Tew D & Handy N, *Chem Phys Lett*, 393 (2004) 51.

46 Perdew J P, Burke K & Ernzerhof M, *Phys Rev Lett*, 77 (1996) 3865.

47 Perdew J P & Wang Y, *Phys Rev B*, 45 (1992) 13244.

48 Foresman J B & Frisch E, *Exploring Chemistry With Electronic Structure Methods*. (Gaussian, Inc., Pittsburgh, USA) 1994, p. 142.

49 Tomasi J, Mennucci B & Cammi R, *Chem Rev*, 105 (2005) 2999.

50 *Gauss View 5.0*, (Gaussian, Inc., Wallingford CT) 2009.

51 Demertzi M A, Hadjikakou S K, Kovala-Demertzi D, Koutsodimou A & Kubicki M, *Helv Chim Acta*, 83 (2000) 2787.

52 Galani A, Demertzis M A, Kubicki M & Kovala-Demertzi D, *Eur J Inorg Chem*, 9 (2003) 1761.

53 Atkins P W, *Physical Chemistry* (Oxford: Oxford University Press) 1998, Chap. 19 & 20.

54 Seddon J M & Gale J D, *Thermodynamics and Statistical Mechanics*, (Cambridge: Royal Society of Chemistry) 2001, Chap. 10, 11 & 12.

55 Berger G, *Comput Theor Chem*, 1010 (2013) 11.

56 Weiner P K, Langridge R, Blaney J M, Schaefer R & Kollman P A, *Proc Natl Acad Sci USA*, 79 (1982) 3754.

57 Politzer P, Laurence P R & Jayasuriya K, *Environ Health Persp*, 61 (1985) 191.

58 Ghomri A & Mekelleche S M, *J Mol Struct (THEOCHEM)*, 941 (2010) 36.

59 Roy R K & Saha S, *Annu Rep Prog Chem, Sect C*, 106 (2010) 118.

60 Xia Y, Yin D, Rong C, Xu Q, Yin D & Liu S, *J Phys Chem A*, 112 (2008) 9970.